# Probabilistic Seismic Hazard Assessment of India

**S. K. Nath and K. K. S. Thingbaijam**
**Indian Institute of Technology, Kharagpur**

*Online material*: Data files for seismogenic source zones (polygons), smoothed-gridded seismicity models, and hazard curves at 0.2° regular grid spacing over the study region.

## INTRODUCTION

Earthquake disasters occur mainly due to the collapse of buildings and structures triggered by ground motions. It is, therefore, important to predict ground-shaking levels in order to determine appropriate building code provisions for earthquake-resistant design of structures. This involves extensive analyses and development of appropriate seismological models; namely, seismogenic sources, seismic site conditions, and ground motion predictions. The hazard products, *viz*. data and maps, constitute important tools for framing public policies toward land-use planning, building regulations, insurance, and emergency preparedness.

In India, several events during the last 100 years, as listed in Table 1, indicate that even moderate earthquakes ($M_W < 7.0$) can cause significant devastation. On one hand, ongoing urbanization and unprecedented population growth have considerably aggravated the prevailing seismic risk. On the other hand, the available seismic hazard maps covering the entire country are about a decade old. Consequently an updated seismic hazard model for the country is imperative and necessitated by new data, recent findings, and methodological improvements. In the present study, we make a case for new probabilistic seismic hazard analysis (PSHA) of India. The fundamental studies have been carried out to deliver the hazard components, including seismogenic source zonation and seismicity modeling in the Indian subcontinent (Thingbaijam and Nath 2011), assessment of site conditions across the country (Nath, Thingbaijam, Adhikari *et al*. 2011), and a suitability test for the ground-motion prediction equations in the regional context (Nath and Thingbaijam 2011).

**TABLE 1**
**Major Earthquake Casualties during 1900–2008 in India and Adjoining Regions**

| Event (YYYYMMDD) | $M_W$ | Epicentral Region | Casualty Report* | |
|---|---|---|---|---|
| | | | Deaths | Building Damage |
| 19050405 | 7.8 | Kangra, northwest Himalayas | 20,000 | — |
| 19340115 | 8.1 | Bihar-Nepal, central Himalayas | 10,700 | — |
| 19350531 | 7.7 | Quetta, Baluchistan | 60,000 | — |
| 19500815 | 8.6 | Indo-china border† | 1,526 | — |
| 19560721 | 6.0 | Anjar, Gujarat | 156 | — |
| 19671210 | 6.3 | Koyna, South India | 177 | — |
| 19880820 | 6.8 | Udayapur, central north India | 700 | over 64000 |
| 19911020 | 6.8 | Uttarkashi, northwest Himalayas | 2,000 | 18000 |
| 19930929 | 6.2 | Latur, South India | 9,500 | — |
| 19970522 | 5.8 | Jabalpur, central India | 39 | — |
| 19990329 | 6.6 | Chamoli, northwest Himalayas | 103‡ | extensive |
| 20010126 | 7.7 | Bhuj, Gujarat | 20,000 | 339000 |
| 20041226 | 9.1 | Sumatra, Indonesia | 22,7000§ | — |
| 20051008 | 7.6 | Kashmir, northwest Himalayas | 86,000 | — |

* Approximate figures as reported by United States Geological Survey and National Geophysical Data Center;
† Commonly referred to as Assam earthquake;
‡ As reported by India Meteorological Department;
§ 10,749 deaths in India

doi: 10.1785/gssrl.83.1.135

These components are integrated to deliver a preliminary model consisting of spatial distributions of peak ground acceleration (PGA) and 5%-damped pseudo spectral acceleration (PSA).

## EARLIER WORKS

Initial attempts at seismic hazard zonation in the country date back to the late 1950s and early 1960s and were mainly based on subjective and deterministic assessments demarcating regions of varying earthquake damage levels, *e.g.*, Tandon (1956), Krishna (1959), and Guha (1962). The current seismic provisions given by the Bureau of Indian Standards (BIS 2002) divide the country into four seismic zones (II, III, IV, and V); zone II is identified with the lowest hazard and zone V with the highest hazard. Basu and Nigam (1977) adopted a probabilistic approach to prepare seismic zonation maps in terms of PGA for a return period of ~100 years. Khattri *et al.* (1984) delivered a hazard map depicting PGA with 10% probability of exceedance in 50 years. Bhatia *et al.* (1999) preformed a probabilistic seismic hazard analysis of India under the Global Seismic Hazard Assessment Program (GSHAP) framework. Sharma and Malik (2006) reported PSHA for northeast India. In the northwestern portion of Gujarat Province, Petersen *et al.* (2004) tested characteristic seismicity models for three fault sources. Jaiswal and Sinha (2007) performed a probabilistic computation of seismic hazard in peninsular India. Mahajan *et al.* (2010) delivered PSHA for the northwestern Himalayas.

Khattri (2006) pointed out that the absence of probabilistic features in the seismic zonation of BIS (2002) was a critical shortcoming. Recent studies also have revealed inadequacies in the current provisions; Das *et al.* (2006) observed that a single zone factor as given by BIS (2002) for entire northeast of India is inaccurate, while Jaiswal and Sinha (2007) reported that hazard in some parts of peninsular India is higher than that given by BIS (2002); a similar observation was made by Mahajan *et al.* (2010) with respect to the northwestern Himalayas. Since the last decade, there have been significant improvements in the understanding of seismogenesis, seismogenic sources, ground shaking, and site characterization. Furthermore, most of the earlier studies did not address the aleatory and epistemic components. Ground-motion variability is recognized as a critical feature (Esteva 1970; Bender 1984; Bommer and Abrahamson 2006) while epistemic uncertainties are generally addressed by employing multiple models (Kulkarni *et al.* 1984; Bommer *et al.* 2005).

## DATA AND METHOD

### Seismogenic Sources and Seismicity Models

Seismic hazard analysis studies are facilitated by appraisal of the underlying seismotectonic regimes. The Indian subcontinent encompasses different seismotectonic provinces as depicted in Figure 1. The tectonically active interplate regions include the Himalayas, southern Tibetan Plateau, Hindukush-Pamir, Sulaiman-Kirthar ranges, Indo-Myanmar arc, and Andaman-Sumatra belt. The Shillong Plateau zone in northeast India is a special case of an "intraplate margin" region associated with active deformations (*e.g.*, Nath and Thingbaijam 2011). On the other hand, peninsular India is delineated as a stable continental region (SCR). The subduction zones include that of Hindukush-Pamir in the northwest, the Indo-Myanmar arc, and the Andaman-Sumatra seismic belt. Subduction interface earthquakes are also observed across the Himalayas and in the northwestern parts of Indian plate boundary.

Thingbaijam and Nath (2011) carried out an extensive study to determine and parameterize the underlying seismogenic source zones in the Indian subcontinent. They employed the earthquake catalog (accessible at http://www.earthqhaz.net/sacat/; Nath, Thingbaijam, and Ghosh 2011) supplemented by records of historical earthquakes (occurring prior to 1900 and as early as A.D. 819), focal mechanism data from the Global Centroid Moment Tensor database and published literature, and palaeoseismicity findings. The fault database, as depicted in Figure 1, has also been employed with the data obtained from the seismotectonic map of India published by the Geological Survey of India (Dasgupta *et al.* 2000), the seismotectonic map of Afghanistan and the adjoining region published by the U.S. Geological Survey (Wheeler and Rukstales 2007) and that given by Wellman (1966), the tectonic map of the Andaman-Sumatra belt given by Curray (1991), and the fault map of Tibet prepared by He and Tsukuda (2003). Thingbaijam and Nath (2011) formulated a layered seismogenic source zonation corresponding to four hypocentral depth ranges (in km): 0–25, 25–70, 70–180, and 180–300. Figure 2 depicts the areal source zones delineated on the basis of seismicity, fault patterns, and similarity in fault-plane solutions. The representative focal mechanism given in the figure for each zone was derived from the weighted average of the known moment tensors (Thingbaijam and Nath 2011; Thingbaijam 2011). The Gutenberg and Richter (GR) parameters for the zones, *i.e.*, *a*-value and *b*-value, were estimated by means of the maximum likelihood method while the maximum earthquakes $m_{max}$ was decided according to results of earlier investigations or the seismicity analysis performed by the authors. The magnitude of completeness $m_c$ of the earthquake catalog has spatiotemporal variations; this is taken care of while estimating the seismicity parameters for each source zone. The earthquakes have been assigned to each source zone according to epicenter location and hypocentral depth. The earthquake occurrences are considered to be random, following a Poissonian distribution. Smoothed seismicity models represented by seismic activity rates at a regular interval of 0.2° were also constructed for threshold magnitudes of $M_W$ 4.5 and $M_W$ 5.5, respectively. The threshold magnitudes correspond to the overall variations in the magnitude of completeness for subcatalogs covering the periods 1964–2008 and 1900–2008, respectively (Nath, Thingbaijam, Ghosh 2011; Thingbaijam 2011). The electronic supplement contains the data files for all the source zones.

### Ground Motion Prediction Equations

We adopt 16 ground motion prediction equations (GMPEs) as listed in Table 2 for the hazard computations. The GMPEs are

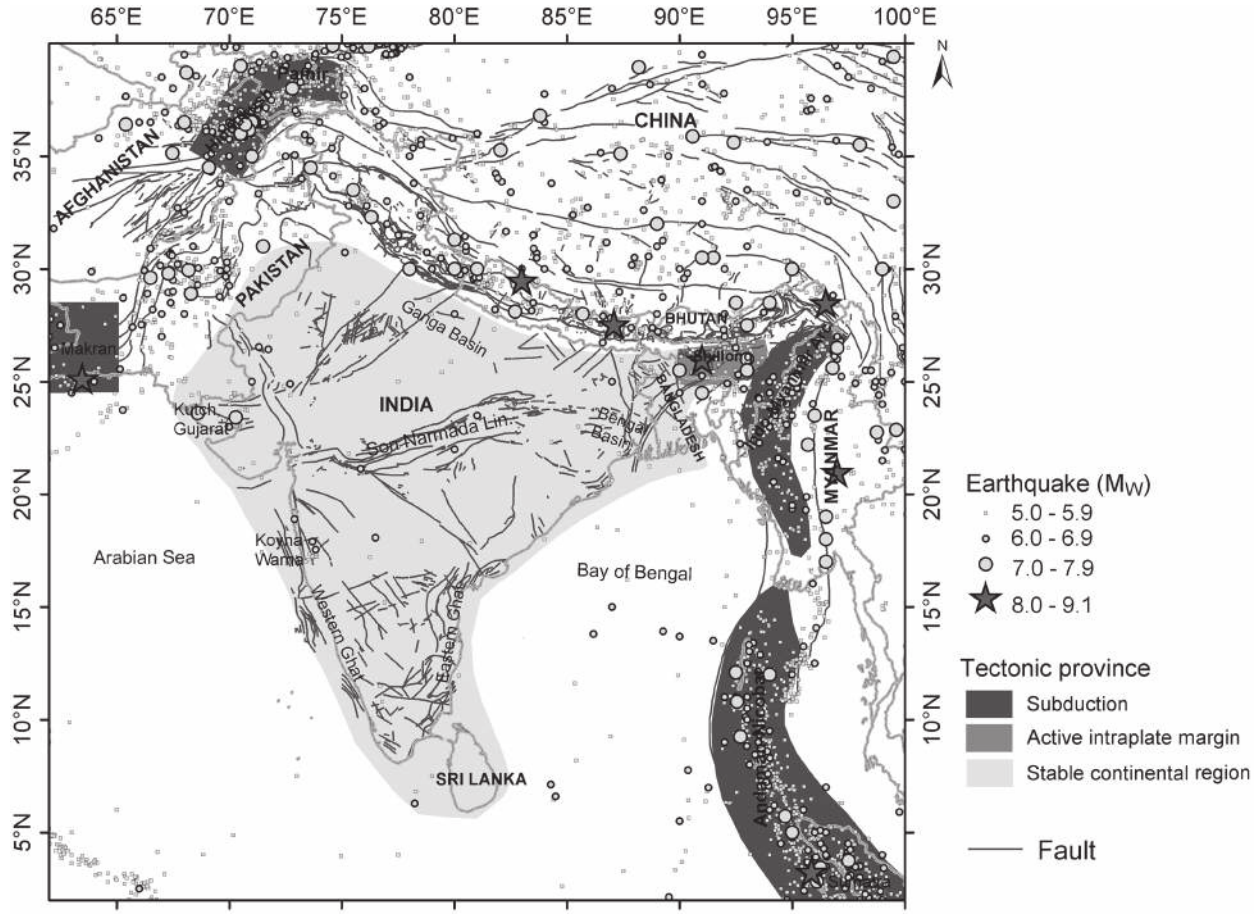


▲ **Figure 1.** A seismicity map of India and adjoining regions depicting epicentral locations of the mainshock events covering the period 819-2008; broadly classified tectonic provinces excluding active shallow crustal and interface regions are delineated with different shades.

selected according to the assessment carried out by Nath and Thingbaijam (2011). A number of candidate GMPEs were selected for the different seismotectonic provinces across India based on the criteria given by Bommer *et al.* (2010) and then subjected to the suitability test proposed by Scherbaum *et al.* (2009). Nath and Thingbaijam (2011) reported that there is general conformity among the GMPEs developed for tectonically active shallow crust while those developed for intraplate regions associating higher ground motions have lower ranks (or suitability), and the subduction zones have significant regional implications. In the present selection, we have included lower-ranked equations such that they are either equally matched or outnumbered by those of higher ranks. Figure 3 depicts the logic tree constructed for the GMPEs in the present analysis. The ranking analyses were carried out using macroseismic intensity data due to which the ranking parameter (*i.e.*, log-likelihood) does not have large variations in several cases (cf., Delavaud *et al.* 2009). Nevertheless, the ranking analysis indicated important considerations to be taken while adopting the relevant GMPEs, such as regional corrections suggested by the developers and elimination due to rather poor conformity. The decision to assign equal weights is taken in order to avoid clear-cut preference. Higher influence by the GPMEs with higher rank collectively, nonetheless, is achieved owing to the selection.

The equations selected for tectonically active shallow crust regions include those of Akkar and Bommer (2010), Boore and Atkinson (2008), Campbell and Bozorgnia (2008), and Sharma *et al.* (2009). The equations developed by Kanno *et al.* (2006) and Zhao *et al.* (2006) address tectonically active shallow crust and subduction zones. For the SCR, the adopted equations include those of Atkinson and Boore (2006), Toro (2002), Raghukanth and Iyengar (2007), and Campbell (2003). In the intraplate margin region of northeast India, the equation developed by Nath, Thingbaijam, Maiti, and Nayak (2011) for the region is included. In order to approximate the associated active deformations, we also include the equation given by Sharma *et al.* (2009).

For the subduction zones, several considerations are imposed according to the observations of Nath and Thingbaijam (2011). The equation developed by Atkinson and Boore (2003) is incorporated with correction for Japan in the case of the Himalayas and northwest India-Eurasia convergence, and with correction for Cascadia in the cases of the Indo-Myanmar and Andaman-Sumatra subduction zones. The equation developed by Atkinson and Macias (2009) is restricted to interface earthquakes with magnitude $M_W \geq 7.5$. Likewise, the equations developed by Gupta (2010) and Lin

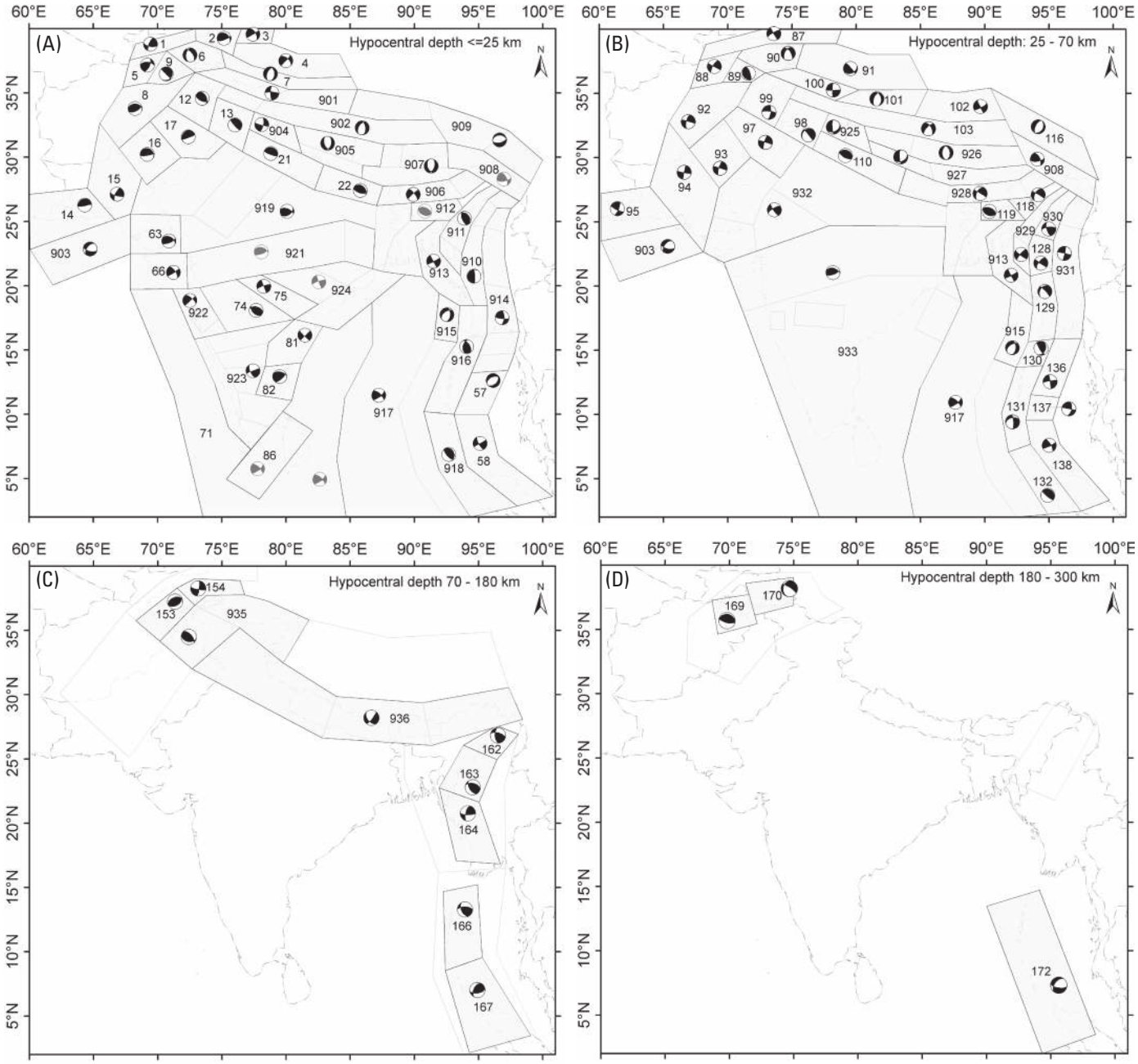


▲ **Figure 2.** The seismogenic source zones demarcated in the Indian subcontinent at different hypocentral depth ranges (after Thingbaijam and Nath 2011).

and Lee (2008) are restricted to intraslab regions of Indo-Myanmar and Himalayas/Hindukush-Pamir, respectively. The equation developed by Youngs *et al.* (1997) based on the world-wide data is also limited to the intraslab-subduction zones.

The adjustments for compatibility between the GMPEs are applied in the same manner as carried out by Nath and Thingbaijam (2011). The mean peak horizontal component of the ground motion is homogenized in terms of new geometric mean definition, namely GMRotI50, as given by Boore *et al.* (2006). The conversion factors given by Beyer and Bommer (2006) and Campbell and Bozorgnia (2008) are used accordingly. The different source-to-site distance measures, namely $R_{JB}$ (Joyner-Boore distance), $R_{EPIC}$ (epicentral distance), $R_{RUP}$ (rupture distance), $R_{HYPO}$ (hypocentral distance), and $R_{CF}$ (distance to the site from center of the fault rupture) for larger earthquakes ($M_W > 6.4$) are calculated by constructing finite-fault models. The predominant focal mechanisms as depicted in Figure 2 are used for this purpose. This approach has been adopted instead of using the relations developed by Scherbaum *et al.* (2004) for tectonically active shallow crustal regions owing to different seismotectonic regimes in the present case. For smaller magnitude earthquakes ($M_W < 6.5$), coincidence is assumed between $R_{JB}$ and $R_{EPIC}$, $R_{RUP}$ and $R_{HYPO}$, and $R_{CF}$ and $R_{HYPO}$, respectively. To estimate the rupture dimensions

**TABLE 2**
**Selected Ground Motion Prediction Equations**

| Tectonic Province | Reference and Code in Brackets |
|---|---|
| Tectonically active shallow crust | Akkar and Bommer 2010 (AKBO10), Boore and Atkinson 2008 (BOAT08), Campbell and Bozorgnia 2008 (CABO08), Sharma *et al.* 2009 (SHAR09) |
| Active shallow crust/ Subduction | Kanno *et al.* 2006 (KAN06), Zhao *et al.* 2006 (ZHAO06) |
| Subduction | Atkinson and Boore 2003 (ATBO03), Atkinson and Macias 2009 (ATMA09), Gupta 2010 (GUPT10)<br>Lin and Lee 2008 (LILE08), Youngs *et al.* 1997 (YOU97) |
| Stable continental region | Toro 2002 (TOR02), Campbell 2003 (CAM03), Atkinson and Boore 2006 (ATBO06), Raghukanth and Iyengar 2007 (RAIY07) |
| Intraplate margin | Toro 2002 (TOR02), Atkinson and Boore 2006 (ATBO06), Sharma *et al.* 2009 (SHAR09), Nath *et al.* 2011 (NATH11) |

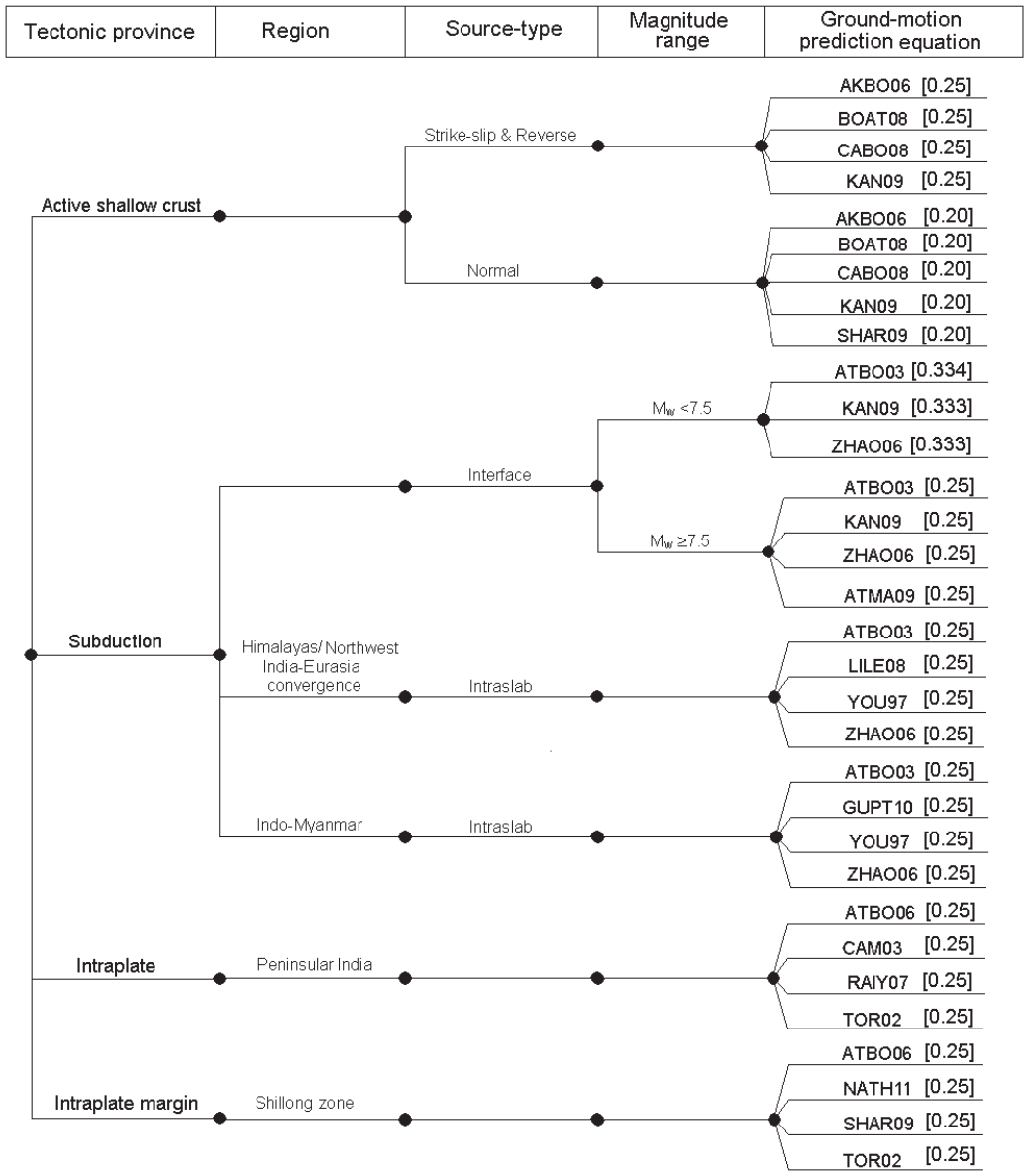


▲ **Figure 3.** The logic tree framework for the ground motion prediction equations; the assigned weights are given inside the square brackets and the references for the codes used for the equations are listed in Table 2.

(*i.e.*, length and width), we use the relations given by Wells and Coppersmith (1994) for crustal events and those given by Strasser *et al.* (2010) for the subduction earthquakes. For the large intraplate earthquakes with reverse faulting, the fault-rupture area estimated from the magnitude is constrained by a factor of 2 (Nath and Thingbaijam 2011). Following the observation of Mai *et al.* (2005) that the hypocenters in strike-slip and crustal dip-slip events mostly occur in deeper sections of the fault plane, the location of hypocenter is placed on the plane decided by 0.5 and 0.8 (reverse faulting), 0.5 and 0.4 (strike-slip faulting), and 0.5 and 0.2 (normal faulting) of the rupture length and width, respectively, from the fault location. The fault location is the top corner of the fault plane such that the dip is on the right-hand side. Depth to shear-wave velocity $V_S$ = 1.0 km/s ($Z_{1.0}$) is estimated using the relation between $Z_{1.0}$ and $V_{S30}$ given by Chiou and Youngs (2008) while depth to $V_S$ = 2.5 km ($Z_{2.5}$) is assigned 2 km following Boore and Atkinson (2008). The computed scenarios consider varying hypocentral depths with homogenous distribution of source-to-site distance not less than 15 km for the shallow crustal zones. This is to avoid estimating ground motions at very near-source locations. Resolving the uncertainty associated with near-source ground motions is currently a topic of active research (Mai 2009). For the lower crust and subduction zones, the minimum hypocentral depths are assigned for the source locations.

## Seismic Site Conditions

Site conditions considered in previous PSHA studies in India discussed earlier include hard rock, rock, and stiff soil conditions. The site classification scheme given by the National Earthquake Hazards Reduction Program (NEHRP) employs average shear-wave velocity for the upper 30 m soil column $V_{S30}$ (Building Seismic Safety Council [BSSC] 2001). Nath, Thingbaijam, Maiti *et al.* (2011) attempted a nationwide assessment of site conditions in India. They observed that ~70% of the total landmass comes under site classes D ($V_{S30}$ ranging between 180 and 360 m/s) and C ($V_{S30}$ ranging between 360 and 760 m/s). In view of the site characterization studies across the country, we consider firm-rock site conditions (standard engineering bedrock) to be more realistic for the regional hazard computations. The standard engineering bedrock conforms to $V_{S30}$~760 m/s (defined as boundary site-class BC). The GMPEs employed in the present analysis are accordingly adopted for the respective site condition uniformly. At the same time, we assume a correction factor of 1 with negligible uncertainty between site-class BC and site-class B (*e.g.*, Boore and Atkinson 2008).

## Computational Framework

In the probabilistic seismic hazard analysis, annual rate of ground motion exceeding a specific value is computed to account for different return periods of the hazard. Contributions from all the relevant sources and possible events are considered. The computational formulation as developed by Cornell (1968), Esteva (1970), and McGuire (1976) is given as follows:

$$\lambda(a>A) = \sum_i \nu_i \int_m \int_r \int_\sigma P(a>A|m,r,\sigma) f_m(m) f_r(r) f_\sigma(\sigma)\, dmdrd\sigma, \quad (1)$$

where $\lambda(a>A)$ is the annual frequency of exceedance of ground motion amplitude $A$, $\nu_i$, is the annual activity rate for $i$th seismogenic source for a threshold magnitude, and function $P$ yields probability of the ground motion parameter $a$ exceeding $A$ for a given magnitude $m$ at source-to-site distance $r$. Also considered is the standard deviation of the residuals (in log-normal distribution) associated with GMPE, denoted by $\sigma$. The corresponding probability density functions are represented by $f_m(m)$, $f_r(r)$, and $f_\sigma(\sigma)$. The probability density function for the magnitudes is generally derived from the GR relation (Gutenberg and Richter 1944). The present implementation makes use of the truncated exponential density function given by Cornell and Vanmarcke (1969),

$$f_m(m) = \frac{\beta \exp[-\beta(m - m_{\min})]}{1 - \exp[-\beta(m_{\max} - m_{\min})]}, \quad (2)$$

where $\beta = b \ln(10)$ and $b$ refers to the $b$-value of GR relation. The distribution is bounded within the minimum magnitude $m_{\min}$ and maximum magnitude $m_{\max}$. Instead of considering probability function for the source-to-site distance measure explicitly, we adopt gridded-point locations within the source zone, wherein finite-fault ruptures are constructed based on the rupture dimensions estimated for each magnitude and the representative focal mechanism as discussed earlier. The seismogenic source is formulated with two schemes; namely, smoothed-gridded seismicity and uniform-seismicity areal zones (or uniformly smoothed). The former entails spatially varying annual activity rates while $b$-value and $m_{\max}$ remain fixed within the source zone. This assumes $b$-value and activity rate to be uncorrelated and a non-uniform distribution of earthquake probability within a zone. On the other hand, the latter postulates each point within the zone to have equal probability for earthquake occurrences.

Ground motion variability constitutes aleatory uncertainty intrinsic to the definition of GMPEs and consequently to that of PHSA. Computations based only on the median ground motions and ignoring the associated variability are known to underestimate the hazards, especially at low annual frequencies of exceedance (Bender 1984; Bommer and Abrahamson 2006). Explicit treatment of the uncertainty is generally achieved by integrating to a number of times the standard deviation; the number of standard deviations is denoted by $\varepsilon$ and its maximum value by $\varepsilon_{\max}$. The ground motions become unrealistically high with increasing $\varepsilon_{\max}$ necessitating truncation at a specific value. We do not explore any technical basis for the selection of $\varepsilon_{\max}$ other than that truncation at $\varepsilon_{\max} < 3$ has been found to be inappropriate (*e.g.*, Bommer and Abrahamson 2006; Strasser *et al.* 2008). The upper bound of the ground motions (or constraining the physical limits on the ground motion values) is a topic of ongoing research (Bommer *et al.* 2004; Strasser and Bommer 2009). The values of $\varepsilon_{\max}$ ranging from 2 to 4 are usually employed (*e.g.*, Bernreuter *et al.* 1989; Romeo and Prestininzi 2000; Marin *et al.* 2004). These aspects allow us to consider $\varepsilon_{\max}$ = 3 to be pragmatic, and the

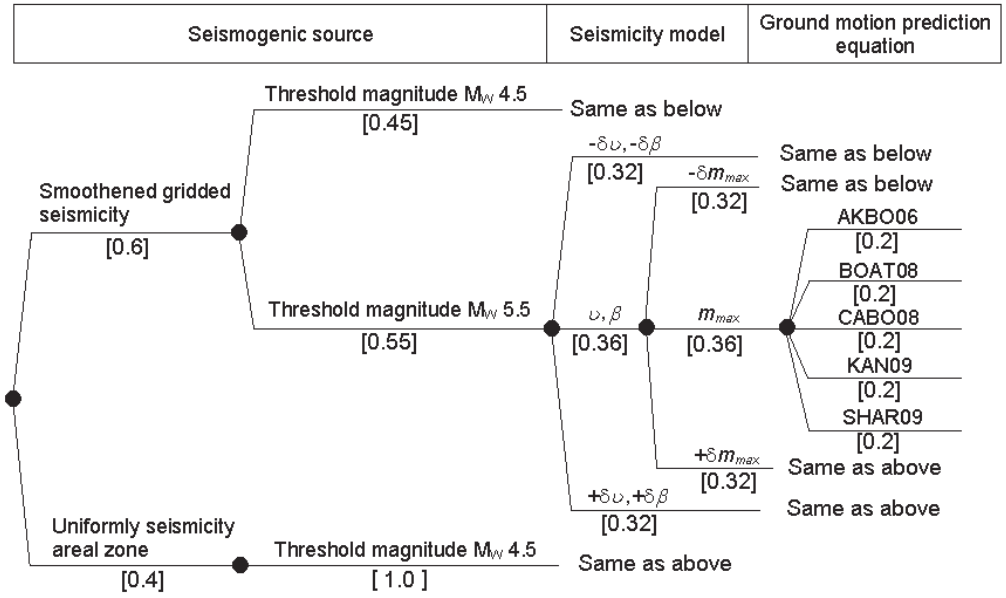


▲ **Figure 4.** A logic tree formulation at a site for the source specified as that of tectonically active shallow crust region with predominant strike-slip faulting; the GPME framework for different tectonic regions is given in Figure 3.

same is accordingly adopted uniformly for all the GMPEs in the present study.

The hazard computation is performed on grid-points covering the entire study region at a spacing of 0.2°. Logic tree framework is employed in the computation at each site to incorporate multiple models in source considerations, GMPEs, and seismicity parameters. Figure 4 depicts a logic tree formulation at a site. In the present study, the seismogenic source framework represented by smoothed-gridded seismicity is collectively assigned weight equal to 0.6. The adopted two models corresponding to the threshold magnitudes of $M_W$ 4.5 and $M_W$ 5.5 are further assigned weights equal to 0.45 and 0.55, respectively. The latter was derived using an earthquake catalog having a longer period compared to the former, and therefore entails higher weight. The seismicity model parameters are assigned weights of 0.36 while the respective ±1 standard deviation gets weight equal to 0.32. Similar weight allotment is assigned to $m_{\max.}$

The computations are performed with the minimum magnitude equal to $M_W$ 4.5. This consideration is corroborated by seismic intensity attenuation models provided by Szeliga *et al.* (2010). The hazard distributions are computed for the source zones at each depth-section separately, and thereafter, integrated.

## RESULTS AND DISCUSSION

### Deliverables

Figure 5 depicts spatial distributions of PGA at 10% probability of exceedance in 50 years estimated for each hypocentral depth-section across active Himalayan tracts and northeast India. The smoothed-gridded seismicity source zonations have been exclusively considered in this case. The hazard contributions from the upper crust zones (0–25 km hypocentral depth range) cover the entire region. In the case of the lower crust zone, *i.e.*, 25–70 km hypocentral depth range, higher hazards are concentrated in two regions: the west-central Himalayas and northeast India. The intraslab earthquakes in the Indo-Myanmar arc occurring in the depth range of 70–180 km constitute a major hazard contributor in northeast India. On the other hand, western parts of Kashmir are exposed to shallow as well as subduction earthquakes. Although not depicted in the figure, hazards from shallow and deep-seated earthquakes can also be noted for the Andaman-Nicobar Islands. The results obtained for each depth range are integrated to establish the overall hazard distribution in the country. Figure 6 depicts the hazard curves obtained at major cities in India; the electronic supplement contains the data files for all the site grid-points.

The seismic hazard maps are presented in Figure 7. These correspond to spatial distribution of PGA and PSA at 0.2 sec and 1 sec computed for 10% and 2% probability of exceedance in 50 years, which correspond to return periods of 475 years and 2,475 years, respectively. In the tectonically active region, higher hazard areas include the extent of the Garhwal Himalayas, parts of western Kashmir, and northeast India. The western Gujarat and Koyna-Warna regions in the stable continental region exhibit higher hazard. Furthermore, regions in and around Delhi, Jabalpur, Satpura, Latur, Bhadrachalam, Ongole, Bangalore, Chennai, Coimbatore, and the Bengal basin have relatively higher hazards.

### Seismic Hazard Perspectives

Table 3 compares the computed PGA with those indicated by BIS (2002), GSHAP, and earlier studies carried out at selected major cities in India. The computation carried out for 10% probability of exceedance in 50 years is considered for the purpose of comparisons. The present study yields comparatively higher hazard, which is pronounced in the high seismogenic regions. Jaiswal and Sinha (2007) estimated lower hazard in the highly

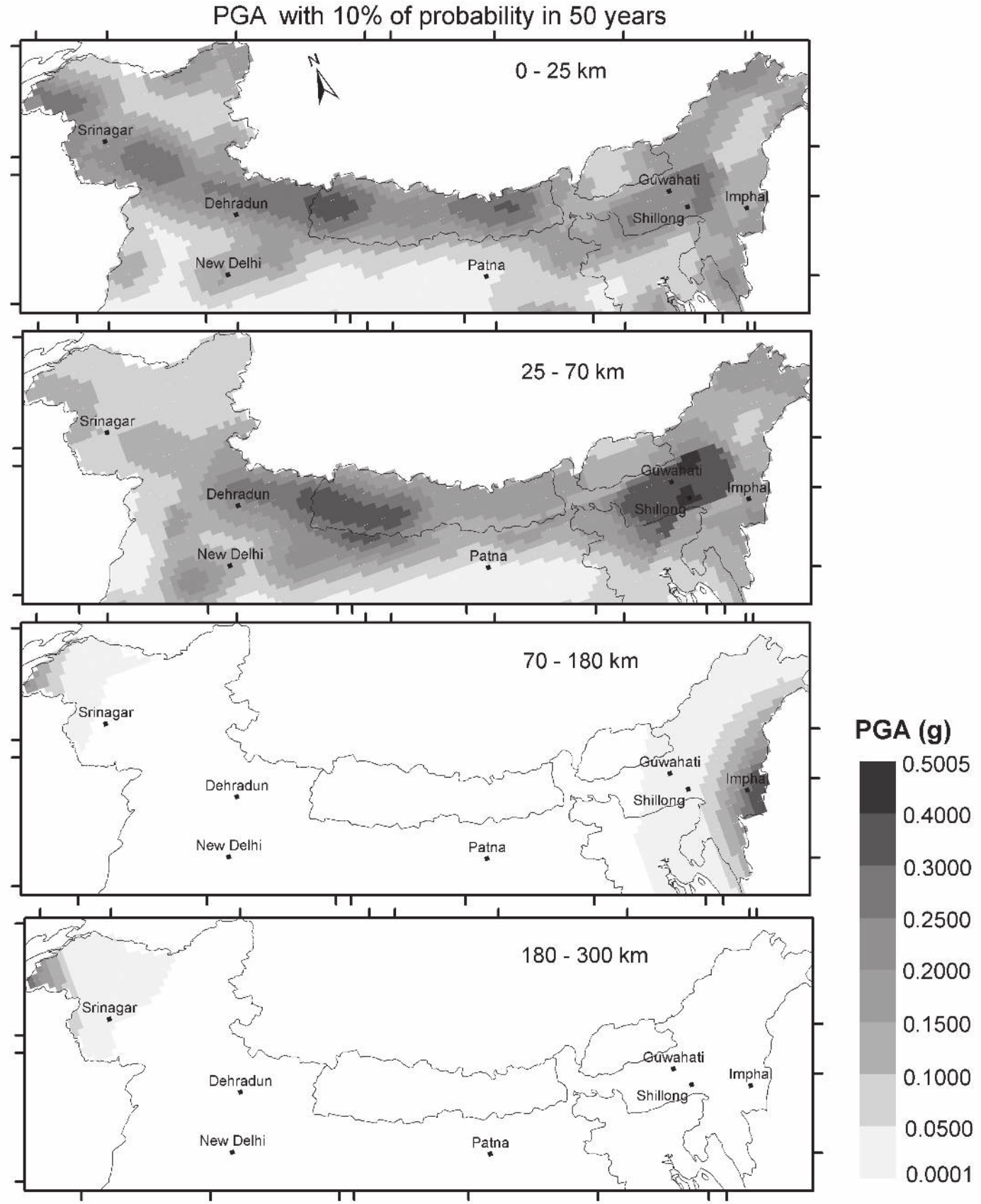


▲ **Figure 5.** The spatial distribution of peak ground acceleration estimated for each hypocentral depth range. The computation corresponds to a return period of 475 years and is exclusively based on smoothed-gridded seismicity source zonations.

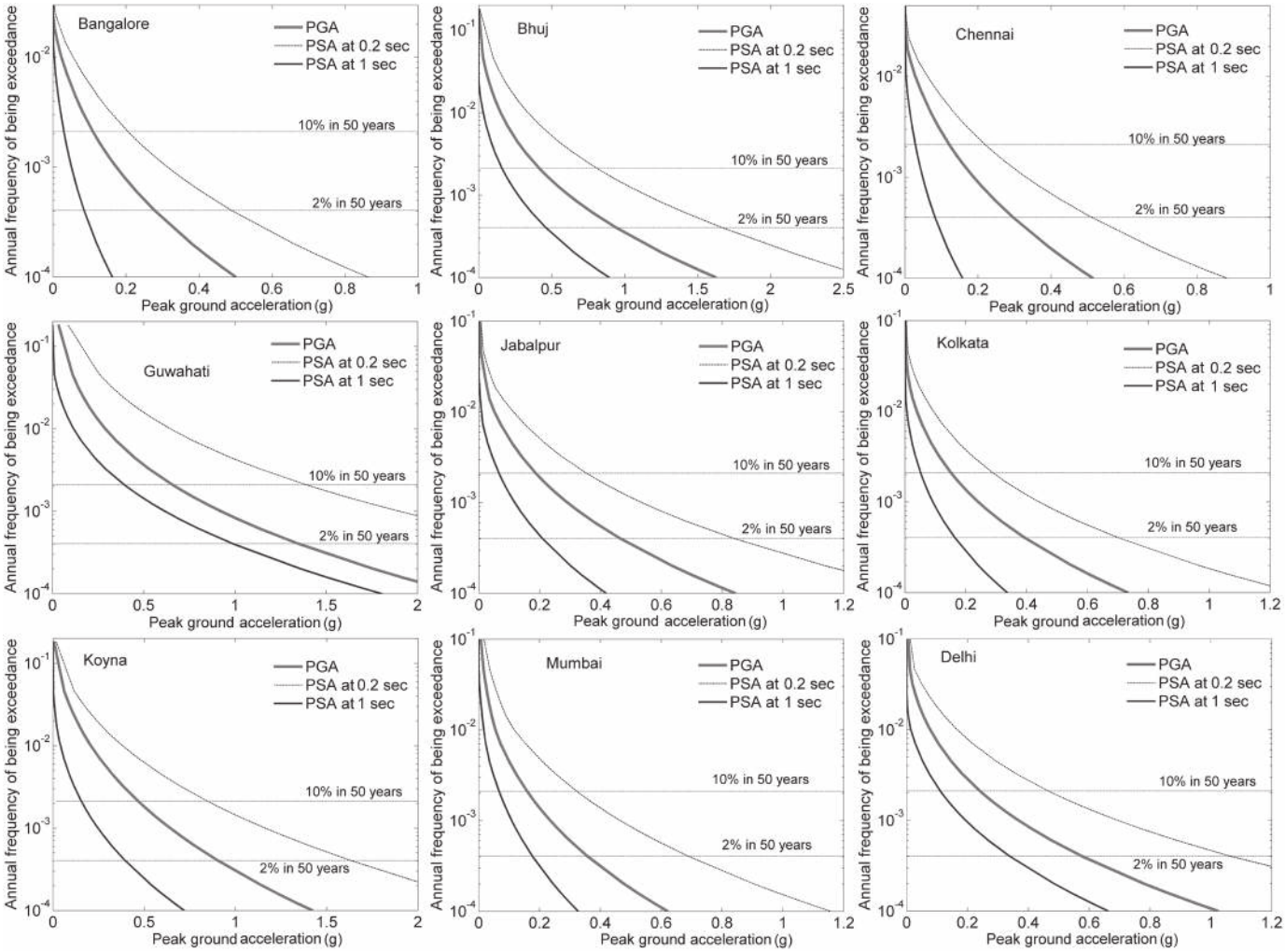


▲ **Figure 6.** The seismic hazard curves for selected cities (as indicated on each plot) computed for PGA and PSA at 0.2 sec and 1 sec, respectively, for uniform firm rock site.

seismogenic zones of Kutch, Gujarat, and Koyna-Warna regions. The same is true of Menon *et al.* (2010) in Tamil Nadu. The present results are, however, similar to those of Anbazhagan *et al.* (2009) in Bangalore. In the northwestern Himalayas, Mahajan *et al.* (2010) estimated maximum PGA as high as 0.75 g. The present analysis associates the region with a maximum of about 0.60 g. In northeast India, the results of the present study are 1.3–2.0 times larger than those of Sharma and Malik (2006).

In order to evaluate the updated seismic hazard analysis *vis-à-vis* the current provisions, we selected eight cities, two of which are located in each of the four specific seismic zones classified by BIS (2002). Figure 8 depicts plots of design response spectra at 5% damping for firm rock site conditions at each city. The PSA at 0.2 sec and 1 sec, respectively, for a 2,475-year return period are employed following the scheme outlined by the International Building Code (IBC 2006, 2009). It is observed that the provision given by BIS (2002) greatly underestimates the hazard distribution. The differences in the estimated hazard distribution compared to the previous studies can be attributed to several factors:

1. In the present study, the GMPEs have been used as appropriate for different seismotectonic regimes. This aspect has been overlooked in most of the earlier studies; for instance Bhatia *et al.* (1999) employed a single equation for the entire country, disregarding the different seismotectonic provinces, and Menon *et al.* (2010) inappropriately employed equations developed for tectonically active regions although their study region falls into the category of stable continental region. More details are given in Nath and Thingbaijam (2011).
2. The layered seismogenic source framework based on hypocentral-depth distribution for the areal zonation, and smoothed-gridded seismicity models employed in the present study, conforms to the variation of seismotectonic attributes with hypocentral depth, especially in subduction zones. This is a significant improvement over the previous studies where seismotectonic attribution has been oversimplified.
3. Multiple models for the seismogenic source and seismicity parameters were not considered in most of the previous

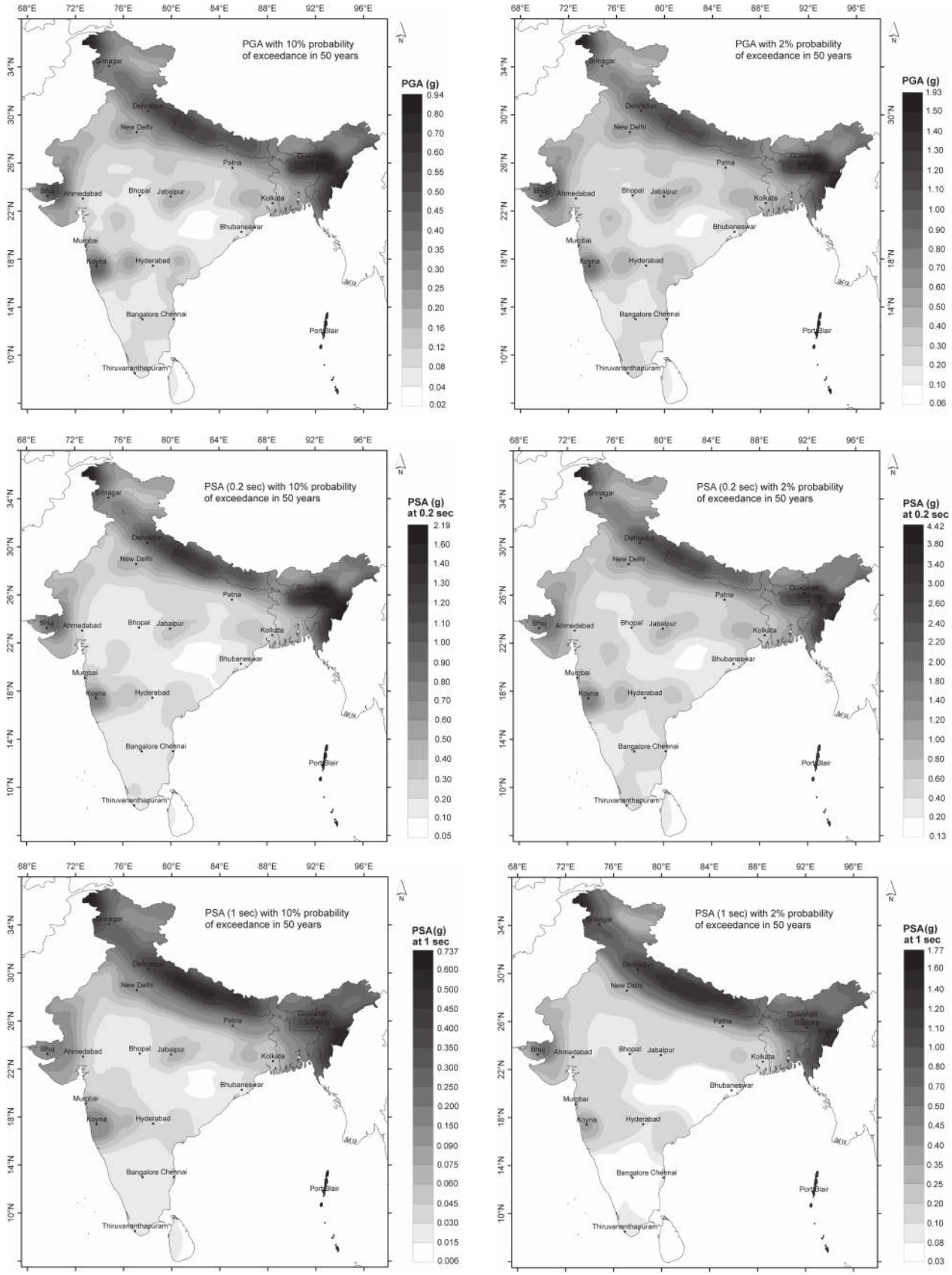


▲ **Figure 7.** Seismic hazard distribution in India in terms of PGA and PSA at 0.2 sec and 0.1 sec for firm rock site conditions. Also included in the maps are the data for Nepal, Bhutan, Bangladesh, and Sri Lanka. The color version of the maps can be accessed on the electronic supplement (Figure S1).

**TABLE 3**

**Estimated peak ground accelerations with 10% probability of exceedance in 50 years at selected major cities across India by Bureau of Indian Standards (BIS 2002), Global Seismic Hazard Assessment Program (GSHAP, Bhatia *et al.* 1999), present study, and other independent studies are listed. Except for BIS and the present study, the PGA estimate is the largest value obtained from the published map contours. The estimate is given for rock site condition or is otherwise indicated.**

| | Peak ground acceleration (g) | | | |
|---|---|---|---|---|
| **City (Latitude, Longitude)** | **BIS (zone)*** | **GSHAP** | **Present study** | **Additional notes** |
| Ahmedabad (23.03°N, 72.61°E) | 0.08 (III) | 0.05 | 0.11 | 0.10 (Jaiswal and Sinha 2007)† |
| Bangalore (12.98°N, 77.58°E) | 0.05 (II) | 0.05 | 0.11 | 0.10 (Jaiswal and Sinha (2007),† 0.15 (Anbazhagan *et al.* 2009) |
| Bhuj (23.25°N, 69.66°E) | 0.18 (V) | 0.20 | 0.42 | 0.25 (Jaiswal and Sinha 2007)† 0.20–0.70 (Petersen *et al.* 2004)‡ |
| Chennai (13.00°N, 80.18°E) | 0.08 (III) | 0.05 | 0.12 | 0.089 (Menon *et al.* 2010), 0.10 (Jaiswal and Sinha 2007)† |
| Dehradun (30.33°N, 78.04°E) | 0.12 (IV) | 0.30 | 0.47 | 0.45 (Mahajan *et al.* 2010) |
| Guwahati (26.18°N, 91.73°E) | 0.18 (V) | 0.30 | 0.66 | 0.50 (Sharma and Malik 2006) |
| Hyderabad (17.45°N, 78.46°E) | 0.05 (II) | 0.05 | 0.09 | 0.08 (Jaiswal and Sinha 2007)† |
| Imphal (24.78°N, 93.94°E) | 0.18 (V) | 0.45 | 0.68 | 0.50 (Sharma and Malik 2006) |
| Jabalpur (23.20°N, 79.95°E) | 0.08 (III) | 0.10 | 0.19 | 0.15 (Jaiswal and Sinha 2007) † |
| Kolkata (22.65°N, 88.45°E) | 0.08 (III) | 0.10 | 0.15 | 0.10 (Jaiswal and Sinha 2007)† |
| Koyna (17.40°N, 73.75°E) | 0.12 (IV) | 0.25 | 0.47 | 0.25 (Jaiswal and Sinha 2007)† |
| Mumbai (19.11°N, 72.85°E) | 0.08 (III) | 0.10 | 0.16 | 0.15 (Jaiswal and Sinha 2007)† |
| New Delhi (28.56°N, 77.11°E) | 0.12 (IV) | 0.15 | 0.24 | — |
| Patna (25.60°N, 85.10°E) | 0.12 (IV) | 0.05 | 0.13 | — |
| Port Blair (11.61°N, 92.72°E) | 0.18 (V) | 0.25 | 0.71 | — |
| Shillong (25.48°N, 92.11°E) | 0.18 (V) | 0.30 | 0.72 | 0.45 (Sharma and Malik 2006) |
| Srinagar (34.08°N, 74.80°E) | 0.18 (V) | 0.25 | 0.33 | — |
| Thiruvananthapuram (8.50°N, 76.95°E) | 0.08 (III) | 0.05 | 0.07 | — |

* After Menon *et al.* (2010)
† Hard rock site;
‡ The authors considered only three fault sources.

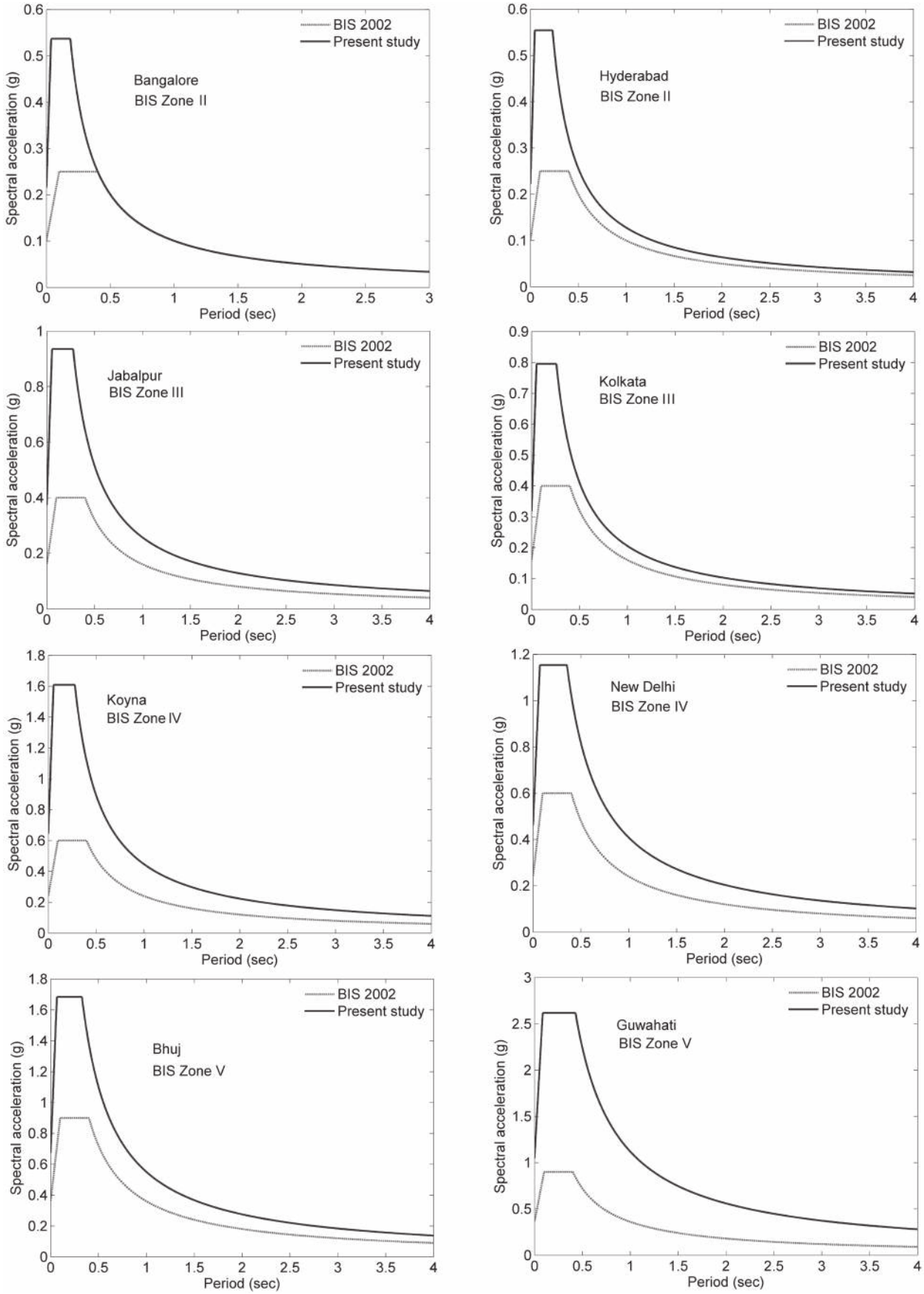


▲ **Figure 8.** Design response spectra (5% damped) for selected cities.

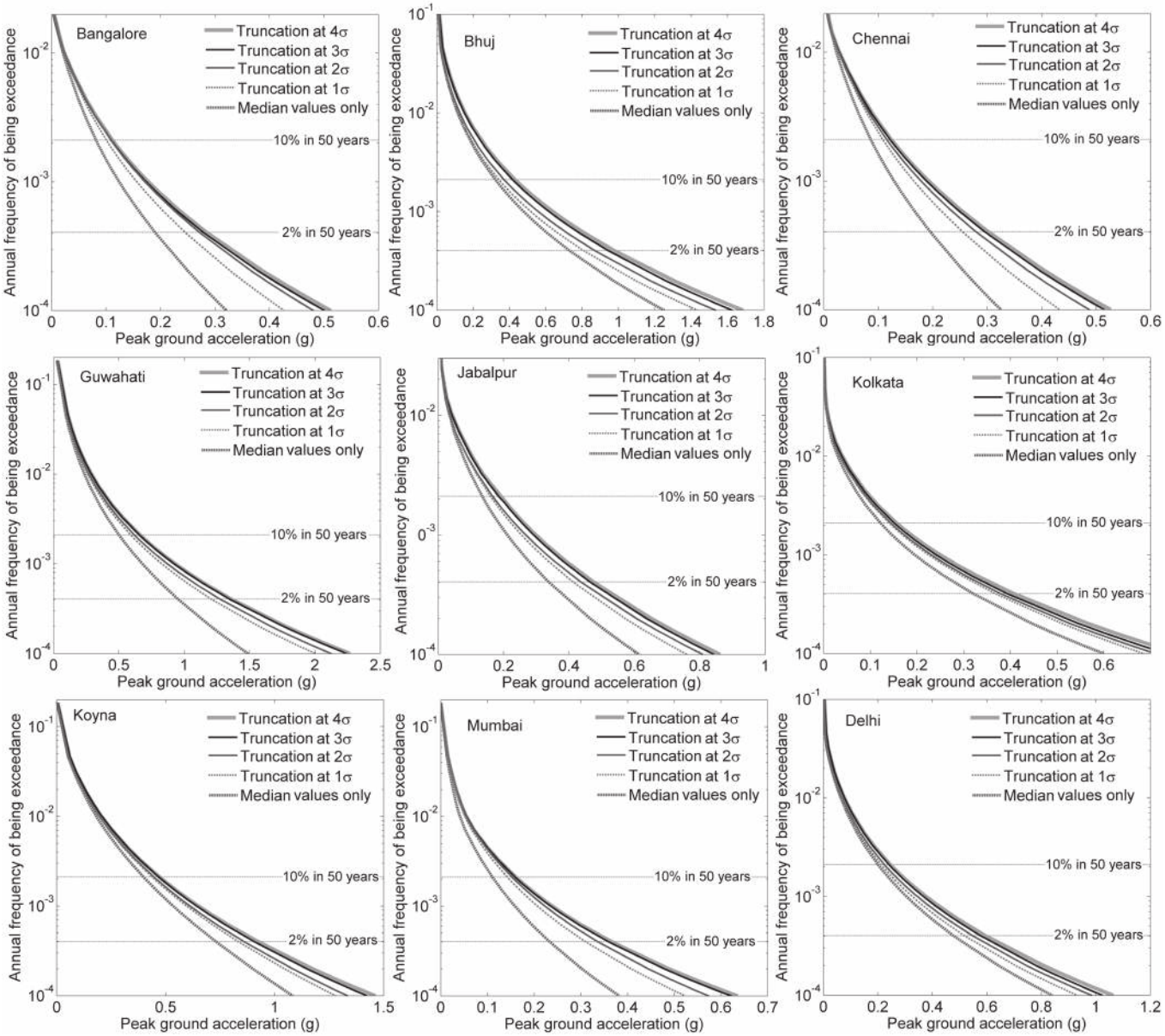


▲ **Figure 9.** Seismic hazard curves for PGA derived using present logic tree formulation with the ground motion truncated at different levels of standard deviation.

studies, except for Jaiswal and Sinha (2007) and Menon *et al.* (2010).

4. The hazard computation in the present study incorporates the ground-motion variability, which incidentally could be a major reason for the estimation of comparatively higher hazard. Previous studies delivered the hazard estimates in terms of median (or mean) ground-motion values. As depicted in Figure 9, the observations at different cities indicate that the median ground-motion values are significantly lower, especially at lower annual exceedance rates.

## CONCLUDING REMARKS

The present study delivers a new-generation probabilistic seismic hazard analysis of India. An attempt has been made to deliver significant improvement in the hazard assessment with incorporation of new data and concepts in seismogenic source considerations, ground motion predictions, and treatment of the associated inherent uncertainties. The hazard distribution has been computed in terms of spectral accelerations at short and long periods, *i.e.*, 0.2 and 1 sec, respectively, which were hitherto unavailable for the entire country. Notwithstanding that further refinement in the hazard computation is warranted from additional features such as fault specific and time-dependent seismicity models, the present results indicate that the hazard distribution in the country is significantly higher than that specified previously by GSHAP and BIS (2002). We envision that the present study will facilitate updating the national building code provisions for earthquake-resistant construction in the country.

## ACKNOWLEDGMENTS

The critical comments and constructive suggestions from Jonathan M. Lees and an anonymous reviewer greatly improved the scientific exposition of the manuscript. KKST is grateful to K. D. Singh, Indian Institute of Technology Guwahati, for the stimulating discussions on design response spectra.

## REFERENCES

Akkar, S., and J. J. Bommer (2010). Empirical equations for the prediction of PGA, PGV, and spectral accelerations in Europe, the Mediterranean region, and the Middle East. *Seismological Research Letters* **81**, 195–s206.

Anbazhagan, P., and T. G. Sitharam (2009). Spatial variability of the depth of weathered and engineering bedrock using multichannel analysis of surface wave method. *Pure and Applied Geophysics* **166**, 409–428.

Anbazhagan, P., J. S. Vinod, and T. G. Sitharam (2009). Probabilistic seismic hazard analysis for Bangalore. *Natural Hazards* **48**, 145–166.

Atkinson, G. M., and D. M. Boore (2003). Empirical ground-motion relations for subduction-zone earthquakes and their application to Cascadia and other regions. *Bulletin of the Seismological Society of America* **93**, 1,703–1,729.

Atkinson, G. M., and D. M. Boore (2006). Earthquake ground-motion predictions for eastern North America. *Bulletin of the Seismological Society of America* **96**, 2,181–2,205.

Atkinson, G. M., and M. Macias (2009). Predicted ground motions for great interface earthquakes in the Cascadia subduction zone. *Bulletin of the Seismological Society of America* **99**, 1,552–1,578.

Basu, S., and N. C. Nigam (1977). Seismic risk analysis of Indian peninsula. In *Proceedings of Sixth World Conference on Earthquake Engineering, New Delhi*. Vol. 1, 782–1,788.

Bender, B. (1984). Incorporating acceleration variability into seismic hazard analysis. *Bulletin of the Seismological Society of America* **74**, 1,451–1,462.

Bernreuter, D. L., J. B. Savy, R. W. Mensing, and J. C. Chen (1989). *Seismic Hazard Characterization of 69 Nuclear Power Plant Sites East of the Rocky Mountains*. U.S. Nuclear Regulatory Commission Report NUREG/CR-5250.

Beyer, K., and J. J. Bommer (2006). Relationships between median values and between aleatory variabilities for different definitions of the horizontal component of motion. *Bulletin of the Seismological Society of America* **96**, 1,512–1,522.

Bhatia, S. C., M. R. Kumar, and H. K. Gupta (1999). A probabilistic seismic hazard map of India and adjoining regions. *Annali di Geofisica* **42**, 1,153–1,166.

Bommer, J. J., and N. A. Abrahamson (2006). Why do modern probabilistic seismic-hazard analyses often lead to increased hazard estimates? *Bulletin of the Seismological Society of America* **96**, 1,967–1,977.

Bommer, J. J., N. A. Abrahamson, F. O. Strasser, A. Pecker, P.-Y. Bard, H. Bungum, F. Cotton, D. Fäh, F. Sabetta, F. Scherbaum, and J. Studer (2004). The challenge of defining upper bounds on earthquake ground motions. *Seismological Research Letters* **75**, 82–95.

Bommer, J. J., J. Douglas, F. Scherbaum, F. Cotton, H. Bungum, and D. Fäh (2010). On the selection of ground-motion prediction equations for seismic hazard analysis. *Seismological Research Letters* **81**, 794–801.

Bommer, J. J., F. Scherbaum, H. Bungum, F. Cotton, F. Sabetta, and N. A. Abrahamson (2005). On the use of logic trees for ground-motion prediction equations in seismic-hazard analysis. *Seismological Research Letters* **95**, 377–389.

Boore, D. M., and G. M. Atkinson (2008). Ground-motion prediction equations for the average horizontal component of PGA, PGV, and 5%-damped PSA at spectral periods between 0.01 s and 10.0 s. *Earthquake Spectra* **24**, 99–138.

Boore, D. M., J. Watson-Lamprey, and N. A. Abrahamson (2006). Orientation-independent measures of ground motion. *Bulletin of the Seismological Society of America* **96**, 1,502–1,511.

Building Seismic Safety Council (BSSC) (2001). *NEHRP Recommended Provisions for Seismic Regulations for New Buildings and Other Structures*. 2000 Edition, Part 1: Provisions, Building Seismic Safety Council for the Federal Emergency Management Agency (Report FEMA 368), Washington, DC.

Bureau of Indian Standards (BIS) (2002). *IS 1893–2002 (Part 1): Indian Standard Criteria for Earthquake Resistant Design of Structures, Part 1–General Provisions and Buildings*. New Delhi: Bureau of Indian Standards.

Campbell, K. W. (2003). Prediction of strong ground motion using the hybrid empirical method and its use in the development of ground-motion (attenuation) relations in eastern North America. *Bulletin of the Seismological Society of America* **93**, 1,012–1,033.

Campbell, K. W., and Y. Bozorgnia (2008). NGA ground motion model for the geometric mean horizontal component of PGA, PGV, PGD and 5% damped linear elastic response spectra for periods ranging from 0.01 to 10s. *Earthquake Spectra* **24**, 139–171.

Chiou, B., and R. R. Youngs (2008). An NGA model for the average horizontal component of peak ground motion and response spectra. *Earthquake Spectra* **24**, 173–215.

Cornell, C. A. (1968). Engineering seismic risk analysis. *Bulletin of the Seismological Society of America* **58**, 1,583–1,606.

Cornell, C. A., and E. H. Vanmarcke (1969). The major influence on seismic risk. *The Fourth World Conference on Earthquake Engineering*, Santiago, Chile, 69–93.

Curray, J. R. (1991). Possible greenschist metamorphism at the base of a 22-km sedimentary section, Bay of Bengal. *Geology* **19**, 1,097–1,100.

Das, S., I. D. Gupta, and V. K. Gupta (2006). A probabilistic seismic hazard analysis of northeast India. *Earthquake Spectra* **22**, 1–27.

Dasgupta, S., P. Pande, D. Ganguly, Z. Iqbal, K. Sanyal, N.V. Venaktraman, S. Dasgupta, B. Sural, L. Harendranath, K. Mazumadar, S. Sanyal, A. Roy, L. K. Das, P. S. Misra, and H. Gupta (2000). *Seismotectonic Atlas of India and Its Environs*. Calcutta: Geological Survey, India.

Delavaud, E., F. Scherbaum, N. Kuehn, and C. Riggelsen (2009). Information-Theoretic Selection of Ground-Motion Prediction Equations for Seismic Hazard Analysis: An Applicability Study Using Californian Data, *Bulletin of the Seismological Society of America* **99**, 3,248–3,263.

Esteva, L. (1970). Seismic risk and seismic design decisions. In *Seismic Design for Nuclear Power Plants*, ed. R. J. Hansen, 142–182. Cambridge, MA: Massachusetts Institute of Technology Press.

Guha, S. K. (1962). Seismic regionalization of India. In *Proceedings of Second Symposium on Earthquake Engineering*, Roorkee, India, 191–207.

Gupta, I. D. (2010). Response spectral attenuation relations for in-slab earthquakes in Indo-Burmese subduction zone. *Soil Dynamics and Earthquake Engineering* **30**, 368–377.

Gutenberg, B., and C. F. Richter (1944). Frequency of earthquakes in California. *Bulletin of the Seismological Society of America* **34**, 185–188.

He, H., and E. Tsukuda (2003). Recent progresses of active fault research in China, *Journal of Geology* **112**, 489–520.

International Building Code (IBC) (2006). *International Building Code*. Club Hills, IL: International Code Council.

International Building Code (IBC) (2009). *International Building Code*. Country Club Hills, IL: International Code Council, Inc.

Jaiswal, K., and R. Sinha (2004). Web portal on earthquake disaster awareness in India; http://www.earthquakeinfo.org.

Jaiswal, K., and R. Sinha (2007). Probabilistic seismic-hazard estimation for peninsular India. *Bulletin of the Seismological Society of America* **97**, 318–330.

Kanno, T., A. Narita, N. Morikawa, H. Fujiwara, and Y. Fukushima (2006). A new attenuation relation for strong ground motion in Japan based on recorded data. *Bulletin of the Seismological Society of America* **96**, 879–897.

Khattri, K. N. (2006). A need to review the current official seismic zoning map of India. *Current Science* **90**, 634–636.

Khattri, K. N., A. M. Rogers, D. M. Perkins, and S. T. Algermissen (1984). A seismic hazard map of India and adjacent areas. *Tectonophysics* **108**, 93–134.

Krishna, J. (1959). Seismic zoning of India. In *Earthquake Engineering Seminar, Roorkee University, India*, 32–38.

Kulkarni, R. B., R. R. Youngs, and K. J. Coppersmith (1984). Assessment of confidence intervals for results of seismic hazard analysis. In *Proceedings, Eighth World Conference on Earthquake Engineering*, vol.1, San Francisco, 263–270.

Lin, P. S., and C. T. Lee (2008). Ground-motion attenuation relationships for subduction-zone earthquakes in northeastern Taiwan. *Bulletin of the Seismological Society of America* **98**, 220–240.

Mahajan, A. K., V. C. Thakur, M. L. Sharma, and M. Chauhan (2010). Probabilistic seismic hazard map of NW Himalaya and its adjoining area, India. *Natural Hazards* **53**, 443–457.

Mai, P. M. (2009). Ground motion: Complexity and scaling in the near field of earthquake ruptures. In *Encyclopedia of Complexity and Systems Science*, ed. R. Meyers, vol. 4, 4,435–4,474.New York: Springer.

Mai, P. M., P. Spudich, and J. Boatwright (2005). Hypocenter locations in finite-source rupture models. *Bulletin of the Seismological Society of America* **95**, 965–980.

Marin, S., J.-P. Avouac, M. Nicolas, and A. Schlupp (2004). A probabilistic approach to seismic hazard in metropolitan France. *Bulletin of the Seismological Society of America* **94**, 2,137–2,163.

McGuire, R. K. (1976). *FORTRAN Computer Program for Seismic Risk Analysis*. USGS Open-File Report 76–67.

Menon, A., T. Ornthammarath, M. Corigliano, and C. G. Lai (2010). Probabilistic seismic hazard macrozonation of Tamil Nadu in southern India. *Bulletin of the Seismological Society of America* **100**, 1,320–1,341.

Nath, S. K., and K. K. S. Thingbaijam (2011). Peak ground motion predictions in India: An appraisal for rock sites. *Journal of Seismology* **15**, 295–315.

Nath S. K., K. K. S. Thingbaijam, M. D. Adhikari, A. Nayak, N. Devaraj, S. K. Ghosh, A. K. Mahajan (2011), Topographic gradient based site characterization in India complemented by strong ground-motion spectral attributes.

Nath, S. K., K. K. S. Thingbaijam, and S. K. Ghosh (2011). A unified earthquake catalogue for South Asia covering the period 1900–2008. Data accessible at http://www.earthqhaz.net/sacat/.

Nath, S. K., K. K. S. Thingbaijam, S. K. Maiti, and A. Nayak (2011). Ground motion predictions in Shillong region, northeast India.

Petersen, M. D., B. K. Rastogi, E. S. Schweig, S. C. Harmsen, and J. S. Gomberg (2004). Sensitivity analysis of seismic hazard for the northwestern portion of the state of Gujarat, India. *Tectonophysics* **390**, 105–115.

Raghukanth, S. T. G., and R. N. Iyengar (2007). Estimation of seismic spectral acceleration in peninsular India. *Journal of Earth System Science* **116,** 199–214.

Romeo, R., and A. Prestininzi (2000). Probabilistic versus deterministic hazard analysis: An integrated approach for siting problems. *Soil Dynamics and Earthquake Engineering* **20**, 75–84.

Scherbaum, F., E. Delavaud, and C. Riggelsen (2009). Model selection in seismic hazard analysis: An information-theoretic perspective. *Bulletin of the Seismological Society of America* **99**, 3,234-3,247.

Scherbaum, F., J. Schmedes, and F. Cotton (2004). On the conversion of source-to-site distance measures for extended earthquake source models. *Bulletin of the Seismological Society of America* **94**, 1,053–1,069.

Sharma, M. L., J. Douglas, H. Bungum, and J. Kotadia (2009). Ground-motion prediction equations based on data from the Himalayan and Zagros regions. *Journal of Earthquake Engineering* **13**, 1,191–1,210.

Sharma, M. L., and S. Malik (2006). Probabilistic seismic hazard analysis and Estimation of spectral strong ground motion on bedrock in northeast India. *Fourth International Conference on Earthquake Engineering, Taipei, Taiwan,* paper no. 15.

Strasser, F. O., M. C. Arango, and J. J. Bommer (2010). Scaling of the source dimensions of interface and intraslab subduction-zone earthquakes with moment magnitude. *Seismological Research Letters* **81**, 941–950.

Strasser, F. O., and J. J. Bommer (2009). Strong ground motions—have we seen the worst? *Bulletin of the Seismological Society of America* **99**, 2,613–2,637.

Strasser, F. O., J. J. Bommer, and N. A. Abrahamson (2008). Truncation of the distribution of ground-motion residuals. *Journal of Seismology* **12**, 79–105.

Szeliga W., S. Hough, S. Martin, and R. Bilham (2010). Intensity, magnitude, location, and attenuation in India for felt earthquakes since 1762. *Bulletin of the Seismological Society of America* **100**, 570–584.

Tandon, A. N. (1956). Zones of India liable to earthquake damage. *Indian Journal of Meteorological Geophysics* **10**, 137–146.

Thingbaijam, K. K. S. (2011). Synoptic modeling for probabilistic seismic hazard analysis of India. PhD thesis, Indian Institute of Technology Kharagpur, India.

Thingbaijam, K. K. S., and S. K. Nath (2011). A seismogenic source framework for Indian subcontinent.

Toro, G. R. (2002). Modification of the Toro *et al.* (1997) attenuation equations for large magnitudes and short distances. Risk Engineering, Inc.: http://www.riskeng.com/PDF/atten_toro_extended.pdf

Wellman, H. N. (1966). Active wrench faults of Iran, Afghanistan and Pakistan, *Geologische Rundschau* **55**, 716–735.

Wells, D. L., and K. J. Coppersmith (1994). New empirical relationships among magnitude, rupture length, rupture width, rupture area, and surface displacement. *Bulletin of the Seismological Society of America* **84**, 974–1,002.

Wheeler, R. L., and K. S. Rukstales (2007). Seismotectonic map of Afghanistan and adjacent areas. U.S. Geological Survey Open-File Report 2007-1104.

Youngs, R. R., S.-J. Chiou, W. J. Silva, and J. R. Humphrey (1997). Strong ground motion relationships for subduction earthquakes. *Seismological Research Letters* **68**, 58–73.

Zhao, J. X., J. Zhang, A. Asano, Y. Ohno, T. Oouchi, T. Takahashi, H. Ogawa, K. Irikura, H. K. Thio, P. G. Somerville, Y. Fukushima, and Y. Fukushima (2006). Attenuation relations of strong ground motion in Japan using site classification based on predominant period. *Bulletin of the Seismological Society of America* **96**, 898–913.

***Department of Geology and Geophysics***
***Indian Institute of Technology Kharagpur***
***Kharagpur 721 302 India***
***nath@gg.iitkgp.ernet.in***
***(S. K. N.)***
***thingbaijam@gmail.com***
***(K. K. S. T.)***